Heat capacity studies of Ce and Rh site substitution in the heavy-fermion antiferromagnet $CeRhIn_5$: Short-range magnetic interactions and non-Fermi-liquid behavior

B. E. Light, Ravhi S. Kumar, and A. L. Cornelius
Department of Physics, University of Nevada, Las Vegas, Nevada 89154-4002, USA

P. G. Pagliuso* and J. L. Sarrao
Materials Science and Technology Division, Los Alamos National Laboratory, Los Alamos, New Mexico 87545, USA
(Received 16 July 2003; published 30 January 2004)

In heavy fermion materials superconductivity tends to appear when long-range magnetic order is suppressed by chemical doping or applying pressure. Here we report heat capacity measurements on diluted alloys of the heavy fermion superconductor $CeRhIn_5$. Heat capacity measurements have been performed on $CeRh_{1-y}Ir_yIn_5$ ($y \leqslant 0.10$) and $Ce_{1-x}La_xRhIn_5$ ($x \leqslant 0.50$) in applied fields up to 90 kOe to study the effect of doping and magnetic field on the magnetic ground state. The magnetic phase diagram of $CeRh_{0.9}Ir_{0.1}In_5$ is consistent with the magnetic structure of $CeRhIn_5$ being unchanged by Ir doping. Doping of Ir in small concentrations is shown to slightly increase the antiferromagnetic transition temperature T_N ($T_N = 3.8$ K in the undoped sample). La doping which causes disorder on the Ce sublattice is shown to lower T_N with no long-range order observed above 0.34 K for $Ce_{0.50}La_{0.50}RhIn_5$. Measurements on $Ce_{0.50}La_{0.50}RhIn_5$ show a coexistence of short-range magnetic order and non-Fermi-liquid behavior. This dual nature of the Ce $4f$ electrons is very similar to the observed results on $CeRhIn_5$ when long-range magnetic order is suppressed at high pressure.

DOI: 10.1103/PhysRevB.69.024419 PACS number(s): 75.30.Kz, 71.18.+y, 71.27.+a

I. INTRODUCTION

Among heavy fermion (HF) materials, magnetically mediated superconductivity has been observed in many materials at the point where long-range order is suppressed by alloying or applying pressure at a quantum critical point (QCP).[1–6] One of these systems, $CeRhIn_5$, is antiferromagnetic (AF) at ambient pressure with $T_N = 3.8$ K and $\gamma \approx 400$ mJ/mol K^2.[6,7] The AF state is suppressed at a pressure of around 1.2 GPa and coexists over a limited pressure range with the superconducting (SC) state.[6,8–10] Recently, HF systems with the formula $CeMIn_5$ (M = Co and Ir) have also been reported to become superconductors at ambient pressure.[11,12] Unlike most HF superconductors, the system $CeRh_{1-y}Ir_yIn_5$ displays a coexistence of AF order and SC state over a wide range of doping ($0.3 < x < 0.6$).[13] Thermodynamic,[7] nuclear quadrupole resonance (NQR),[14] and neutron-scattering[15,16] experiments all show that the electronic and magnetic properties of $CeRhIn_5$ are anisotropic in nature.

To better understand the magnetic ground state out of which SC evolves, we have performed heat capacity measurements on both the $CeRh_{1-y}Ir_yIn_5$ ($y \leqslant 0.10$) and $Ce_{1-x}La_xRhIn_5$ ($x \leqslant 0.50$) systems. The magnetic-field studies for various dopings are an extension of our previous work.[7,17] The measurements were performed along both the tetragonal a and c axes in applied magnetic fields to 90 kOe. The dependence of the magnetic transitions with respect to temperature, magnetic field applied along different crystal directions, and doping using heat capacity measurements allows the determination of the magnetic interactions in these complicated materials. Precisely determining the changes of magnetic properties with different variables gives insight into favorable conditions for magnetically mediated superconductivity. Field-induced transitions when the magnetic field is applied along the a direction are seen in all samples that display AF order. A detailed phase diagram for $CeRh_{0.9}Ir_{0.1}In_5$ shows excellent agreement to that of the undoped parent compound $CeRhIn_5$ suggesting that Ir doping does not change the AF order from the measured incommensurate spin-density wave.[14–16] La doping suppresses magnetic order with the $x = 0.50$ sample showing no long-range AF order; however, a coexistence of short-range magnetic order and non-Fermi-Liquid (NFL) behavior is observed.

Though a great deal of both experimental and theoretical work have been performed on heavy fermion systems, a general understanding of the crossover from the single impurity to the lattice limits has been elusive. Recently, the observance of multiple energy scales[18,19] and the coexistence of localized and delocalized f electrons[20,21] have shown the necessity of including the lattice and considering the localization of f electrons in heavy fermion systems. Our results on $Ce_{0.50}La_{0.50}RhIn_5$, which is near the QCP, show signatures of the coexistence of short-range (short-range magnetic order) and long-range (non-Fermi-liquid) behavior. We find a striking resemblance of the results on $Ce_{0.50}La_{0.50}RhIn_5$ to those on $CeRhIn_5$ driven to a QCP under pressure.[8]

II. EXPERIMENT

$CeRh_{1-y}Ir_yIn_5$ and $Ce_{1-x}La_xRhIn_5$ single crystals were grown by a self-flux technique.[22] The samples were found to crystallize in the primitive tetragonal $HoCoGa_5$-type structure[23,24] with lattice parameters, determined by x-ray diffraction, in agreement with literature values.[13,22] Heat capacity measurements, using a standard thermal relaxation method, were performed in a quantum design PPMS system equipped with a superconducting magnet capable of generating a 90 kOe magnetic field. The lat-

tice heat capacity was determined by measuring $LaRhIn_5$ which has no f electrons. The $LaRhIn_5$ data were subtracted from $Ce_{1-x}La_xRh_{1-y}Ir_yIn_5$ to obtain the magnetic heat capacity C_m. This makes the assumption that the specific heat of the lattice is unchanged by the substitutions. Since the lattice constants change less than 0.6% for the studied samples[13,17] one expects that the Debye temperature, which is known to depend on volume, and hence the lattice contribution to the heat capacity remains constant for our purposes.

III. RESULTS AND DISCUSSION

A. Low-temperature specific heat

The low-temperature specific-heat measurements were performed over the temperature range $0.34\ \mathrm{K} < T < 20\ \mathrm{K}$ in applied magnetic fields to 90 kOe. As previously mentioned, the lattice contribution to the heat capacity is subtracted using $LaRhIn_5$ as a reference compound. The total magnetic specific heat can be written as

$$C_m = C_{elec} + C_{order} + C_{hyp}, \tag{1}$$

where C_{elec} is the electronic contribution, C_{order} is from magnetic correlations (short and long ranged) between the Ce $4f$ electrons, and C_{hyp} is from the nuclear moment of the In atoms. The electronic contribution is given by γT for $T > T_N$ and $\gamma_0 T$ for $T < T_N$, where $\gamma > \gamma_0$. In the magnetically ordered samples below T_N, as done before,[7] we use the form

$$C_{order} = \beta_M T^3 + \beta'_M (e^{-E_g/k_B T}) T^3, \tag{2}$$

where $\beta_M T^3$ is the standard AF magnon term and the second term is an activated AF magnon term. The need for an activated term to describe heat capacity data has been seen before in other Ce and U compounds,[7,25–27] and rises from an AF spin-density wave (SDW) with a gap in the excitation spectrum due to anisotropy. The $CeRhIn_5$ magnetic structure indeed displays an anisotropic SDW with modulation vector (1/2,1/3,0.297) (Refs. 15,16) which is consistent with this picture. The In atoms have a nuclear magnetic moment which gives rise to hyperfine contribution to the heat capacity C_{hyp}. C_{hyp} is given by A/T^2 with A given by the relation[28]

$$A = \frac{R}{3}\left(\frac{I+1}{I}\right)\left(\frac{\mu H_{hyp}}{k_B}\right)^2, \tag{3}$$

where I is the nuclear moment (9/2 for In), μ is the nuclear magnetic moment (5.54 μ_N for In), and H_{hyp} is the magnitude of the internal field strength at the In site that can be due to both internal H_{int} and externally applied H fields.

Data for $CeRhIn_5$ in a 90 kOe magnetic field applied along the tetragonal a axis ($H \| a$) is shown in Fig. 1. Two phase transitions at $T_N = 3.91$ K and $T_1 = 3.09$ K are clearly seen. T_N is the transition to long-range AF order, and T_1 is a first-order field-induced magnetic phase transition.[29] Field-induced transitions have been observed before in $CeRhIn_5$,[30] and this topic will be discussed in detail later. The upturn at low temperatures is due to the In nuclear Schottky term.

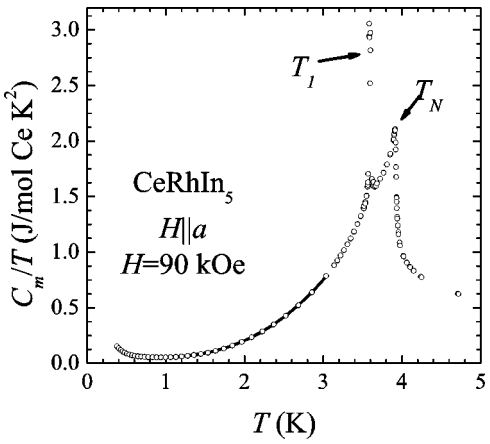

FIG. 1. Magnetic heat capacity C_m divided by temperature T vs T measured on $CeRhIn_5$ in an applied magnetic field of 90 kOe with $H \| a$. Two phase transitions T_N and T_1 correspond to the antiferromagnetic ordering temperature and a field-induced transition. The solid line for $T < 0.8\ T_N$ represents a fit to the data as described in the text.

Note that we are in the high temperature limit for the nuclear Schottky term and use the high-temperature approximation [Eq. (3)] that the nuclear heat capacity falls off as T^{-2}. The solid line in Fig. 1 is a fit to Eq. (1) with $\gamma_0 = 38 \pm 2$ mJ/mol Ce K^2, $\beta_M = 6.3 \pm 0.2$ mJ/mol Ce K^4, $\beta'_M = 310 \pm 20$ mJ/mol Ce K^4, $E_g/k_B = 4.4 \pm 0.2$ K. Fits like this were successful for all $CeRh_{1-y}Ir_yIn_5$ samples in all applied fields directed along either the a or c axis. However, fits to the $Ce_{1-x}La_xRhIn_5$ data, at least for $x > 0.03$, did not give satisfactory results due to short-range order and non-Fermi-liquid effects and only the $x = 0$ and $x = 0.03$ data were fit and will be reported.

B. Magnetic entropy

The magnetic entropy S_m can be found by integrating C_m/T as a function of temperature. This has been done for all of the measured samples and the results in zero applied field are shown in Fig. 2.

All of the measured samples approach $R \ln 2$ by 20 K with the exception of the $Ce_{0.50}La_{0.50}RhIn_5$ sample (which is still very close to $R \ln 2$). Application of a magnetic field has a nearly negligible effect on the measured entropy for all samples with again the exception of the $Ce_{0.50}La_{0.50}RhIn_5$ sample. The reason for the differences in the behavior of the $Ce_{0.50}La_{0.50}RhIn_5$ sample relative to the others will be explained in detail later but is due, at least in part, to non-negligible entropy below 0.35 K that we cannot measure. It is also possible that the stoichiometry is slightly less than the nominal starting value of $x = 0.50$. In fact a value of $x = 0.47$ gives an entropy of $R \ln 2$ at 20 K. For the rest of the paper, we will assume that $x = 0.50$. However, using $x = 0.47$ has little effect on the data and would not change our conclusions. The observance of $R \ln 2$ entropy in all of the measurements is indicative that the measured C_m values are due solely to a doublet crystal-field (CF) ground state. This is consistent with other studies which show the lowest CF level

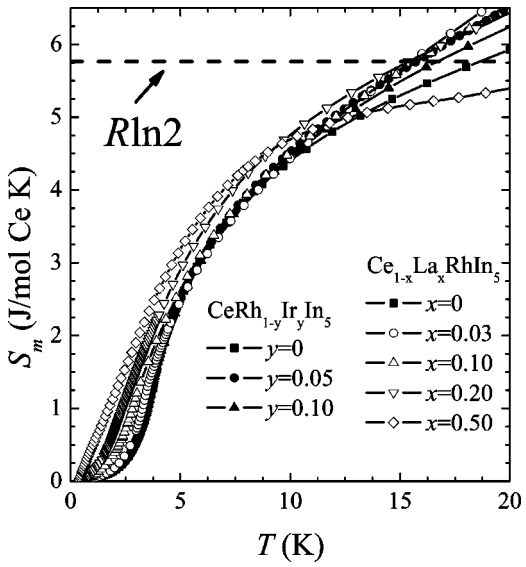

FIG. 2. Magnetic entropy S_m, found by integrating C_m/T, measured on doped $CeRhIn_5$ samples. All of the samples approach $R\ln 2$ of entropy by 20 K consistent with a $S=1/2$ doublet crystal-field ground state.

is a doublet separated by 60–80 K from the first excited level.[31–33] Thus we are confident that our measurement of C_m are solely due to the Ce $4f$ electrons in a $S=1/2$ doublet CF ground state.

C. Magnetic order

Neutron-diffraction studies have shown that the substitution of 10% La for Ce lowers T_N from 3.8 K found in $CeRhIn_5$ to 2.7 K but does not change the SDW ground state.[34] As mentioned, $CeRh_{1-y}Ir_yIn_5$ displays a coexistence of AF order and SC state over a wide range of doping ($0.3<y<0.6$).[13] As it has been established that two-dimensional (2D) magnetic ground states favor SC,[35] it is important to determine if the SC state arises out of the known SDW ground state of the undoped sample. Figure 3 shows the zero-field data as a function of Ir doping.

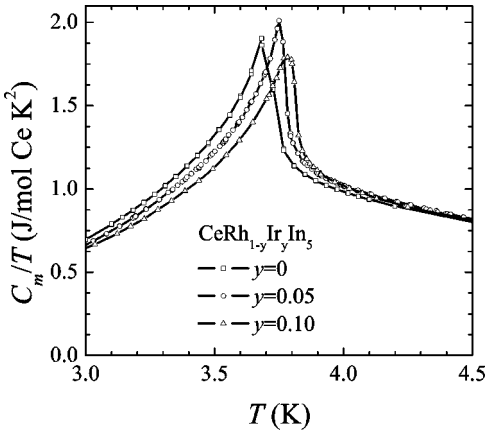

FIG. 3. Magnetic heat capacity C_m divided by temperature T versus T measured on $CeRh_{1-y}Ir_yIn_5$ in zero field. The value of T_N increases as y increases.

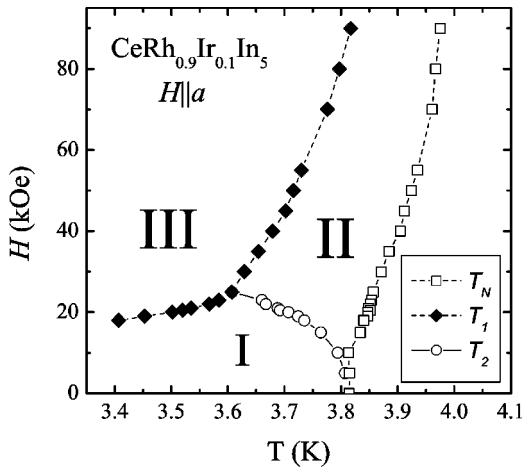

FIG. 4. The cumulative phase diagrams for $CeRh_{0.9}Ir_{0.1}In_5$ in various applied fields H applied along the a axis. T_N corresponds to the antiferromagnetic ordering temperature, and T_1 and T_2 correspond to field-induced first- and second-order transitions, respectively. The dashed lines are guides to the eyes.

The application of a magnetic field alters the magnetic interactions. As reported before for $CeRhIn_5$,[30] when $H\|c$, T_N decreases for all of the samples that show AF order as is usually seen in heavy fermion systems.[36] As shown in Fig. 1, for $H\|a$ field-induced magnetic transitions are observed in $CeRh_{0.9}Ir_{0.1}In_5$. A cumulative H-T phase diagram is shown in Fig. 4.

T_N corresponds to the antiferromagnetic ordering temperature, and T_1 and T_2 correspond to field-induced first- and second-order transitions, respectively. The dashed lines are guides to the eyes. The similarity to the phase diagram of the undoped $CeRhIn_5$ is remarkable.[30] This naturally leads to the conclusion that the Ir substitution does not change the magnetic structure (incommensurate SDW) of $CeRhIn_5$ at least for $x\leqslant 0.10$. In a manner similar to the effect of doping, recent neutron-scattering results show that the incommensurate SDW only weakly changes with pressure up to 2.3 GPa.[37] As stated previously, the magnetic structure in regions I and II is a spin-density wave that is incommensurate with the lattice where region II has a larger magnetic moment on each Ce atom; region III corresponds to a spin-density wave that is commensurate with the lattice.[38]

Taken along with neutron-scattering experiments on $Ce_{0.9}La_{0.1}RhIn_5$ that show no change in the magnetic structure,[34] substitutions of up to 10% of La for Ce and 10% Ir for Rh do not change the magnetic structure. This result leads one to believe that the superconductivity in the Ir doped samples and NFL behavior in the La doped samples evolve out of the magnetic structure of the ground state, namely, an incommensurate SDW. However, recent neutron-scattering results on Ir doped samples with $y\geqslant 0.30$ show the appearance of a commensurate component to the magnetic order.[38]

D. Long-range magnetic order

All of the $CeRh_{1-y}Ir_yIn_5$ data and $Ce_{0.97}La_{0.03}RhIn_5$ were fit using Eqs. (1)–(3) for $T<0.8T_N$. Fits were made in ap-

TABLE I. Summary of the fitting parameters to the $Ce_{1-x}La_xRh_{1-y}Ir_yIn_5$ data. Definitions of the various coefficients are given in the text. The units are kOe for H, mJ/mol Ce K^2 for γ, mJ/mol Ce K^4 for β_M and β'_M, K for E_g/k_B, mJ K/mol Ce for A. The number in parentheses is the statistical uncertainty in the last digit from the least-squares fitting procedure.

x	y	H	γ_0	β_M	β'_M	E_g/k_B	H_{int}
0	0	0	50(3)	19(1)	510(30)	7.0(4)	2
0	0	50($\|c$)	45(2)	24(1)	580(30)	7.4(4)	56(2)
0	0	90($\|c$)	41(2)	29(1)	600(30)	7.2(4)	97(1)
0	0	50($\|a$)	38(2)	19(1)	390(30)	5.8(4)	54(1)
0	0	90($\|a$)	38(2)	6(2)	310(30)	4.4(2)	94(1)
0	0.05	0	48(2)	23(1)	710(40)	8.2(4)	2
0	0.05	50($\|c$)	44(2)	26(1)	650(40)	7.9(4)	59(2)
0	0.05	90($\|c$)	42(7)	31(5)	750(180)	8.1(9)	98(4)
0	0.05	50($\|a$)	27(7)	30(5)	580(90)	7.6(7)	57(1)
0	0.05	90($\|a$)	32(8)	15(7)	360(40)	5.2(6)	99(1)
0	0.10	0	81(4)	15(3)	420(60)	6.5(4)	2
0	0.10	50($\|c$)	64(3)	27(2)	600(50)	8.0(4)	57(4)
0	0.10	90($\|c$)	56(3)	33(2)	680(70)	8.1(4)	98(1)
0	0.10	50($\|a$)	55(3)	25(2)	410(40)	6.7(4)	57(3)
0	0.10	90($\|a$)	38(2)	6(2)	310(30)	4.4(2)	94(2)
0.03	0	0	43(2)	38(1)	500(34)	6.7(2)	2
0.03	0	50($\|c$)	34(3)	47(2)	650(160)	7.6(8)	60(2)
0.03	0	90($\|c$)	34(2)	50(2)	530(50)	6.6(3)	99(3)
0.03	0	50($\|a$)	24(3)	38(3)	360(40)	5.4(4)	65(2)
0.03	0	90($\|a$)	25(4)	20(3)	330(90)	4.2(2)	102(3)

plied fields of 50 kOe and 90 kOe applied along both the a and c axes. A summary of the results is displayed in Table I. The internal field H_{int} was found by using the measured A value and using Eq. (3). From NQR measurements, it is known that in the absence of an applied field the internal field at the In sites in $CeRhIn_5$ is of the order of 2 kOe,[14] which is consistent with the data in Table I, where H_{int} for the 50 and 90 kOe data is slightly higher than the applied field. For the zero-field data, a value of 2 kOe for H_{int} gives a nearly negligible contribution to the heat capacity in our temperature range so we have set $H_{int}=2$ kOe for $H=0$ in all of our fits shown in Table I (this assumption has a negligible effect on the zero-field fit parameters as they do not change if $H_{int}=0$ is used). For all values of y the value of γ_0 is seen to decrease as field is applied as usually seen in heavy fermion systems.[36] For $H\|c$ the value of β_M is seen to increase as field is applied while E_g/k_B remains relatively constant. For AF systems where $\beta_M \propto D^{-3}$ with D the spin-wave stiffness,[28] one would expect D to decrease in an applied field that weakens AF interactions leading to an increase in β_M. For $H\|a$ in an applied field, the values of β_M and E_g/k_B tend to decrease relative to the zero-field value. As seen in Fig. 1, the fits to the data in this direction are for $T<T_1$ where the spin structure is believed to be a SDW that is commensurate with the lattice. As the zero-field spin structure is an incommensurate SDW, the commensurate state has a smaller value of E_g/k_B as one would naively expect. The small amount of La doping decreases the value of γ_0 as

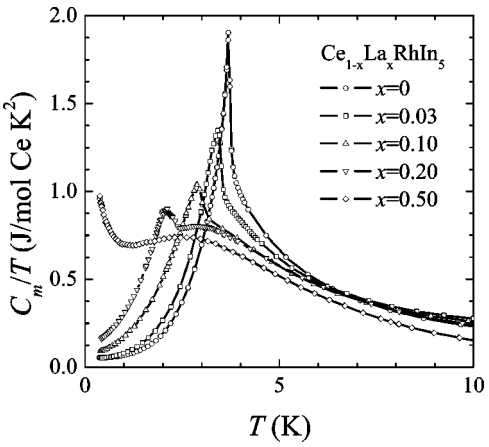

FIG. 5. Magnetic heat capacity C_m divided by temperature T vs T measured on $Ce_{1-x}La_xRhIn_5$ in zero field.

expected. Qualitatively, applied field affects the fitting parameters for the La doped sample in the same manner as the Ir doped samples. For $H\|c$ the value of β_M is seen to increase with E_g/k_B remaining unchanged within the uncertainty of the values, while for $H\|a$, the values of β_M and E_g/k_B both decrease as field increases.

E. Short-range magnetic order

As shown in a previous report, La doped for Ce in $Ce_{1-x}La_xRhIn_5$ suppresses T_N and leads to a QCP for $x \approx 0.40$, a value consistent with the 2D percolation threshold.[17] The zero field data for various values of x ($x \leqslant 0.5$) are shown in Fig. 5.

These results are in good agreement with previous La doped[17,39] and Y doped[40] reports. The value of T_N is seen to decrease as x increases indicative of a weakening of the magnetic interactions. For $x=0.50$, the upturn at low temperatures is not due to magnetic order but can be fit quite well for $T<0.7$ K to a non-Fermi-liquid form $C/T=\gamma^* \ln T^*/T$.[41,42] In all samples, a significant portion of the entropy ($\sim R \ln 2$ as shown in Fig. 2) is found above T_N. This is consistent with neutron-scattering results that show short-range magnetic correlations at temperatures on the order of $2T_N$.[43] The contribution to the heat capacity from these short-range correlations can be seen as a ''hump'' in the heat capacity data that becomes apparent as T_N is suppressed and is consistent with our previous report that speculated the hump was due to short-range magnetic interactions.[17]

To further discuss the data in terms of short-range magnetic interactions, we consider the results of McCoy and Wu for a 2D Ising model on a square lattice with two magnetic interaction energies E_1 and E_2.[44] We identify E_1 and E_2 as E_{in} and E_{out} (in-plane and out-of-plane directions) that correspond to the magnetic interaction energies along the two orthogonal directions, where this mapping is completely rigorous of some concern as the model only takes into account nearest-neighbor interactions on a 2D lattice, and the inclusion of both a magnetic interaction in the c direction along with next-nearest neighbors would lead to multiple magnetic interaction strengths. However, to a first approximation, it

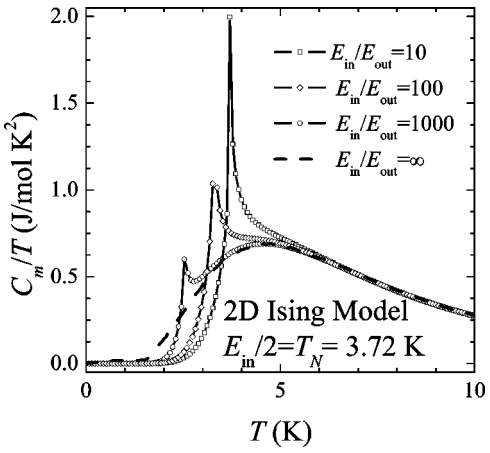

FIG. 6. Magnetic heat capacity C_m divided by temperature T vs T as calculated for the 2D Ising model described in the text. E_{in} and E_{out} correspond to the magnetic interaction energies in orthogonal directions. $E_{in}/2$ has been fixed to the value of $T_N=3.72$ K of $CeRhIn_5$. The curves represent various values of E_{out}.

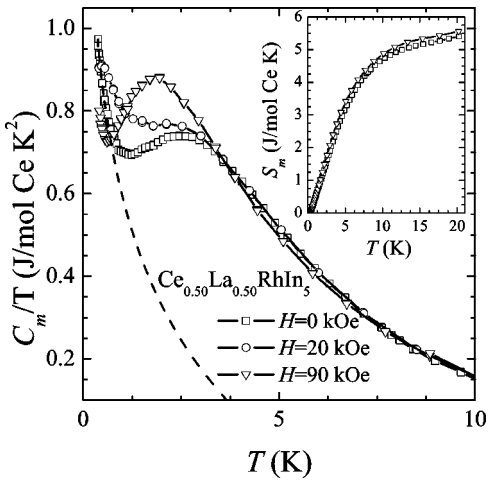

FIG. 7. Magnetic heat capacity C_m divided by temperature T vs T measured on $Ce_{0.50}La_{0.50}RhIn_5$ in various applied fields. The dashed line shows the non-Fermi-liquid contribution to the heat capacity for the zero-field data as described in text. The inset shows the measured entropy up to 20 K at 0 and 90 kOe.

seems reasonable to qualitatively describe our data using E_{in} as the interaction in the basal plane and E_{out} as the out-of-plane (interlayer) interaction. We fix $E_{in}/2=T_N$ and vary E_{out} with the results shown in Fig. 6.

The $E_{in}/E_{out}=10$ curve looks remarkably similar to the $CeRhIn_5$ data shown in Fig. 5 showing a peak in C_m/T at T_N. Neutron-scattering results on $CeRhIn_5$ show the magnetic correlation lengths above T_N are only about a factor of 2–3 different for measurements along and perpendicular to the c axis,[43] and magnetic-susceptibility measurements show a factor of 2–3 difference in the in-plane and out-of-plane susceptibility.[31–33,40] However, as there are more near neighbors (4) in plane than out of plane (2) using the value of 10 for E_{in}/E_{out} seem reasonable from a qualitative point of view. Keeping E_{in} fixed and reducing E_{out} is seen to have a dramatic effect on C_m/T as T_N moves to lower temperatures and a Schottky-like maximum (or hump) appears. In the calculations, the heat capacity for the case $E_{in}/E_{out}=\infty$ shows no long-range order and is identical to that of a two-state Schottky anomaly with an energy difference of E_{in} between the two levels. The evolution of the 2D Ising calculation displays the same systematics as the data taken on $Ce_{1-x}La_xRhIn_5$ shown in Fig. 5. In this scenario, as La is doped for Ce, short-range in-plane magnetic correlations remain while those along the c axis are weakened considerably by the disorder. This culminates in the observance of no long-range order for $x=0.50$.

F. Non-Fermi-liquid behavior

As mentioned, the heat capacity appears to display NFL behavior in the $x=0.50$ sample that is near the QCP. This is in agreement with the La doped results of Kim *et al.*[39] and Y doped results of Zapf *et al.*[40] who find NFL behavior near the QCP in the magnetic susceptibility, heat capacity, and resistivity (Y only) data. To further investigate the NFL behavior in the La doped system, data in numerous magnetic fields were collected, and some of the results are displayed in Fig. 7.

As mentioned previously, the zero-field data can be fit quite well for $T<0.7$ K to a NFL logarithmic dependence. The application of an applied field moves the NFL feature to higher temperatures eventually appearing to merge with the hump centered around 2.5 K in zero field (note that the upturn at the lowest temperature for the 90 kOe applied field is due to the In nuclear term). The inset to Fig. 7 shows the measured entropy up to 20 K at 0 and 90 kOe. Note that there is a small increase in the entropy which approaches the expected $R\ln 2$ (5.76 J/mol Ce K) as field is increased. This ''missing'' entropy is due to the large increase in C_m/T at low temperatures due to the NFL behavior that we do not measure; if we could measure to lower temperature, we would expect to find all of the $R\ln 2$ entropy observed for other samples (see Fig. 2).

In heavy fermion systems, there is a natural competition between single-site and intersite interactions. This has lead to a scenario of two types of coexisting f electrons: a local ''Kondo gas'' and a global ''Kondo liquid.''[20,21,45] In a similar fashion, we can separate the data in Fig. 7 into two components: a ''localized'' term due to short-range order C_{SRO} (the hump) and a NFL term C_{NFL} that can be attributed to intersite effects. It is important to note that the C_m/T data in Fig. 7 is nearly field independent above 5 K. Above 5 K, we would expect the NFL contribution to be negligible as T^* in the equation $C_{NFL}/T=\gamma^*\ln T^*/T$ is of the order of 5 K. Therefore, we assume that there is a field independent term C_{SRO} which we find by subtracting off the zero-field NFL contribution. The resulting C_{SRO} is displayed in Fig. 8.

The data can be fit reasonably well by the 2D Ising model with a value of $E_{in}/2=2.64$ K and only around 2/3 of the Ce spins being involved. These numbers are similar to those obtained on Y doped samples.[40] However, Zapf *et al.*[40] interpret their data in terms of crystal fields that also display Schottky-like behavior. As mentioned previously, the heat capacity in the 2D Ising model for the case $E_{in}/E_{out}=\infty$ is identical to that of a two-state Schottky anomaly.[44] The fact

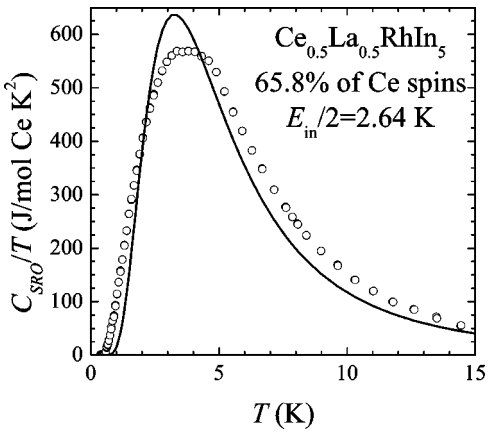

FIG. 8. Magnetic heat capacity due to short-range magnetic order C_{SRO} divided by temperature T vs T measured on $Ce_{0.50}La_{0.50}RhIn_5$. The solid line is a fit to the data involving 65.8% of the Ce spins as described in the text.

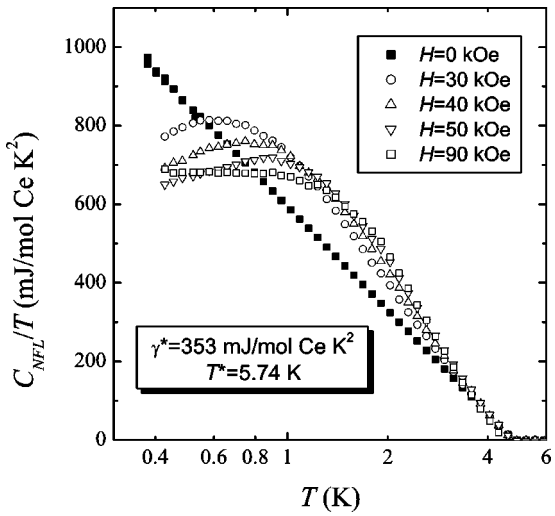

FIG. 9. Measured non-Fermi-liquid heat capacity C_{NFL} divided by temperature T vs T measured on $Ce_{0.50}La_{0.50}RhIn_5$ in various applied fields. The zero-field data is given by $\gamma^* \ln T^*/T$ with $\gamma^* = 353$ mJ/mol Ce K^2 and $T^* = 5.7$ K.

that the data is broader than the fit is likely due to disorder. McCoy and Wu have indeed shown that disorder broadens measured features in heat capacity measurements.[44] The value of $E_{in}/2$ is less than the value of T_N for the undoped sample that is used in Fig. 6. As already discussed, doping nonmagnetic La atoms should not only reduce E_{out} as was done in Fig. 6, it should also reduce E_{in} as we observe. The short-range order scenario also gives a natural explanation of the absence of magnetic-field effects on the C_{SRO} data because the spins align in the basal plane and the magnetic field is applied perpendicular to the spins. The magnetic field would be expected to have an effect on E_{out} while leaving E_{in} unchanged. Since $E_{out} \ll E_{in}$ the ratio of E_{in}/E_{out} will be quite large and the heat capacity data are very insensitive to changes in E_{out} as long as the ratio is large, and C_{SRO} appears Schottky-like in nature peaking at the same temperature since E_{in} is not changing. The C_{SRO} data are also similar to that seen by others near the QCP for La doping,[39] Y doping,[40] and applied pressure.[8]

The case of high pressure is of particular interest, because the hump like feature is seen in the undoped stoichiometry near the QCP when pressure is applied.[8] Though Fisher *et al.* attribute the hump to the Kondo effect,[8] the feature is much too narrow to be fit by a spin 1/2 Kondo impurity model.[46] In fact the feature due to superconductivity is seen below a maximum in C that is field independent as is our C_{SRO} data. In this interpretation, the long-range 3D magnetic order is nearly destroyed while short-range 2D magnetic correlations are still present near the QCP. This could easily be envisioned by the magnetic correlation length becoming smaller along the c axis than the nearest-neighbor Ce-Ce separation which is much greater than the basal plan Ce-Ce distances leading to very large values of E_{in}/E_{out}. For the 16.5 kbar data of Fisher *et al.* that is very near the QCP, the data are fit fairly well assuming that 65% of the Ce spins are involved in the magnetic-heat capacity with an energy of $E_{in}/2 = 2.45$ K. These numbers are remarkably similar to the $Ce_{0.5}La_{0.5}RhIn_5$ data that is near the QCP. The small feature near 2.5 K in the pressure data could be explained by AF order with the fit parameters listed. This would mean that the superconducting transition would be at even lower temperatures (perhaps the very small looking feature in the data at 1 K).[8] Recent NQR results at 16 kbar are interpreted in terms of microscopic regions of AF order below around 2.8 K and AF and superconducting states below 1.3 K.[10] This scenario is in excellent agreement with the above analysis. The application of higher pressure would be expected to increase the anisotropy of the magnetic interactions while reducing the magnitude of $E_{in}/2$. This is exactly what is found at 19 kbar where the data are fit reasonably well by $E_{in}/2 = 1.88$ K with $E_{in}/E_{out} = \infty$. Unlike the crystal-field interpretation,[40] the universality of the humplike feature near the QCP in both pressure and doping experiments, the agreement with the 2D Ising calculations, and the fact that the crystal-field levels are found not to change with La doping in $CeCoIn_5$ compounds[20] lead us to confidently conclude that the data we have labeled C_{SRO} are indeed due to short-range magnetic order.

The remaining $\sim 34\%$ of the entropy for the $x = 0.50$ sample is found in a NFL $\gamma^* \ln T^*/T$ term. After the nuclear In term is estimated using Eq. (3) with $H_{int} = H$ and subtracted along with the field independent C_{SRO}/T contribution, the remaining data is C_{NFL}/T. The C_{NFL}/T data is plotted for various fields in Fig. 9.

As field increases, the low-temperature data appears to go to a nearly constant Fermi-liquid-like value. This field dependent behavior is remarkably similar to that seen in one of the prototypical NFL system $CeCu_{5.9}Au_{0.1}$,[41] and also to recent results on $CeCoIn_5$.[47] These findings lead to the conclusion that the $4f$ electrons in $Ce_{0.5}La_{0.5}RhIn_5$ display both short-range (short-range magnetic order) and long-range (non-Fermi-liquid) behavior consistent with an evolving picture of coexisting short- and long-range correlations in the Kondo lattice.[20,21,45]

IV. CONCLUSIONS

In conclusion, we have measured the heat capacity on both the $CeRh_{1-y}Ir_yIn_5$ ($y \leq 0.10$) and $Ce_{1-x}La_xRhIn_5$ (x

$\leqslant 0.50$) systems. Field-induced transitions when the magnetic field is applied along the *a* direction for $CeRh_{0.90}Ir_{0.10}In_5$ are very similar to those observed in $CeRhIn_5$ suggestive that Ir doping up to 10% does not change the AF order from the measured incommensurate spin-density wave in the undoped sample.[15] La doping suppresses magnetic order with the $x=0.50$ sample showing no long range AF order. The La-doped data shows excellent agreement to calculation on a 2D square Ising lattice with La doping weakening the out-of-plane magnetic interactions. In $Ce_{0.50}La_{0.50}RhIn_5$, a coexistence of short-range magnetic order and non-Fermi-liquid behavior is observed that is remarkably similar in nature to the pressure induced superconductivity at a QCP in undoped $CeRhIn_5$.[8] This ''dual'' nature of the $4f$ electrons in Ce based and other heavy fermion systems shows the importance of including the effect of the lattice when studying these systems.

ACKNOWLEDGMENTS

Work at UNLV is supported by U.S. Department of Energy EPSCoR-State/National Laboratory Partnership Grant No. DE-FG02-00ER45835 and Cooperative Agreement Grant No. DE-FC08-98NV1341. Work at LANL is performed under the auspices of the U.S. Department of Energy.

*Present address: Instituto de Fsic ''Gleb Wataghin''-UNICAMP, 13083-970 Campinas, Brazil.

[1] F. Steglich, J. Aarts, C.D. Bredl, W. Lieke, D. Meschede, W. Franz, and H. Schäfer, Phys. Rev. Lett. **43**, 1892 (1979).
[2] D. Jaccard, K. Behina, and J. Sierro, Phys. Lett. A **163**, 475 (1992).
[3] R. Movshovich, T. Graf, D. Mandrus, J.D. Thompson, J.L. Smith, and Z. Fisk, Phys. Rev. B **53**, 8241 (1996).
[4] F.M. Grosche, S.R. Julian, N.D. Mathur, and G.G. Lonzarich, Physica B **223-224**, 50 (1996).
[5] N.D. Mathur, F.M. Grosche, S.R. Julian, I.R. Walker, D.M. Freye, R.K. Haselwimmer, and G.G. Lonzarich, Nature (London) **394**, 39 (1998).
[6] H. Hegger, C. Petrovic, E.G. Moshopoulou, M.F. Hundley, J.L. Sarrao, Z. Fisk, and J.D. Thompson, Phys. Rev. Lett. **84**, 4986 (2000).
[7] A.L. Cornelius, A.J. Arko, J.L. Sarrao, M.F. Hundley, and Z. Fisk, Phys. Rev. B **62**, 14 181 (2000).
[8] R.A. Fisher, F. Bouquet, N.E. Phillips, M.F. Hundley, P.G. Pagliuso, J.L. Sarrao, Z. Fisk, and J.D. Thompson, Phys. Rev. B **65**, 224509 (2002).
[9] T. Mito, S. Kawasaki, G.q. Zheng, Y. Kawasaki, K. Ishida, Y. Kitaoka, D. Aoki, Y. Haga, and Y. Onuki, Phys. Rev. B **63**, 220507(R) (2001).
[10] T. Mito, S. Kawasaki, Y. Kawasaki, G.-Q. Zheng, Y. Kitaoka, D. Aoki, Y. Haga, and Y. Onuki, Phys. Rev. Lett. **90**, 077004 (2003).
[11] C. Petrovic, P.G. Pagliuso, M.F. Hundley, R. Movshovich, J.L. Sarrao, J.D. Thompson, Z. Fisk, and P. Monthoux, J. Phys.: Condens. Matter **13**, L337 (2001).
[12] C. Petrovic, R. Movshovich, M. Jaime, P.G. Pagliuso, M.F. Hundley, J.L. Sarrao, Z. Fisk, and J.D. Thompson, Europhys. Lett. **53**, 354 (2001).
[13] P.G. Pagliuso, C. Petrovic, R. Movshovich, D. Hall, M.F. Hundley, J.L. Sarrao, J.D. Thompson, and Z. Fisk, Phys. Rev. B **64**, 100503(R) (2001).
[14] N.J. Curro, P.C. Hammel, P.G. Pagliuso, J.L. Sarrao, J.D. Thompson, and Z. Fisk, Phys. Rev. B **62**, R6100 (2000).
[15] W. Bao, P.G. Pagliuso, J.L. Sarrao, J.D. Thompson, Z. Fisk, J.W. Lynn, and R.W. Erwin, Phys. Rev. B **62**, R14621 (2000).
[16] W. Bao, P.G. Pagliuso, J.L. Sarrao, J.D. Thompson, Z. Fisk, J.W. Lynn, and R.W. Erwin, Phys. Rev. B **67**, 099903(E) (2003).
[17] P.G. Pagliuso, N.O. Moreno, N.J. Curro, J.D. Thompson, M.F. Hundley, J.L. Sarrao, Z. Fisk, A.D. Christianson, A.H. Lacerda, B.E. Light, and A.L. Cornelius, Phys. Rev. B **66**, 054433 (2002).
[18] A.L. Cornelius, J.M. Lawrence, T. Ebihara, P.S. Riseborough, C.H. Booth, M.F. Hundley, P.G. Pagliuso, J.L. Sarrao, J.D. Thompson, M.H. Jung, A.H. Lacerda, and G.H. Kwei, Phys. Rev. Lett. **88**, 117201 (2002).
[19] T. Ebihara, E.D. Bauer, A.L. Cornelius, J.M. Lawrence, N. Harrison, J.D. Thompson, J.L. Sarrao, M.F. Hundley, and S. Uji, Phys. Rev. Lett. **90**, 166404 (2003).
[20] S. Nakatsuji, S. Yeo, L. Balicas, Z. Fisk, P. Schlottmann, P.G. Pagliuso, N.O. Moreno, J.L. Sarrao, and J.D. Thompson, Phys. Rev. Lett. **89**, 106402 (2002).
[21] S. Nakatsuji, D. Pines, and Z. Fisk, cond-mat/0304587 (unpublished).
[22] E.G. Moshopoulou, Z. Fisk, J.L. Sarrao, and J.D. Thompson, J. Solid State Chem. **158**, 25 (2001).
[23] Y.N. Grin, Y.P. Yarmolyuk, and E.I. Gladyshevskii, Kristallografiya **24**, 242 (1979) [Sov. Phys. Crystallogr. **24**, 137 (1979)].
[24] Y.N. Grin, P. Rogl, and K. Hiebl, J. Less-Common Met. **121**, 497 (1986).
[25] C.D. Bredl, J. Magn. Magn. Mater. **63-64**, 355 (1987).
[26] N.H. van Dijk, F. Bourdarot, J.P. Klaasse, I.H. Hagmusa, E. Bruck, and A.A. Menovsky, Phys. Rev. B **56**, 14 493 (1997).
[27] S. Murayama, C. Sekine, A. Yokoyanagi, and Y. Onuki, Phys. Rev. B **56**, 11 092 (1997).
[28] M.R. Lees, O.A. Petrenko, G. Balakrishnan, and D.M. Paul, Phys. Rev. B **59**, 1298 (1999).
[29] The software used to measure the heat capacity uses average values to fit the thermal relaxation data. From the raw traces, the transitions which we have assigned as first order are clearly first order in nature. Experience tells us the averaging method underestimates the value of the heat capacity near the peak of the first-order transition by a factor of 4 or 5.
[30] A.L. Cornelius, P.G. Pagliuso, M.F. Hundley, and J.L. Sarrao, Phys. Rev. B **64**, 144411 (2001).
[31] T. Takeuchi, T. Inoue, K. Sugiyama, D. Aoki, Y. Tokiwa, Y. Haga, K. Kindo, and Y. Onuki, J. Phys. Soc. Jpn. **70**, 877 (2001).
[32] P.G. Pagliuso, N.J. Curro, N.O. Moreno, M.F. Hundley, J.D. Thompson, J.L. Sarrao, and Z. Fisk, Physica B **320**, 370 (2002).
[33] A.D. Christianson, J.M. Lawrence, P.G. Pagliuso, N.O. Moreno, J.L. Sarrao, J.D. Thompson, P.S. Riseborough, S. Kern, E.A. Goremychkin, and A.H. Lacerda, Phys. Rev. B **66**, 193102 (2002).
[34] W. Bao, A.D. Christianson, P.G. Pagliuso, J.L. Sarrao, J.D. Th-

ompson, A.H. Lacerda, and J.W. Lynn, Physica B **312-313**, 120 (2002).
[35] P. Monthoux and G.G. Lonzarich, Phys. Rev. B **63**, 054529 (2001).
[36] G.R. Stewart, Rev. Mod. Phys. **56**, 755 (1984).
[37] A. Llobet, J.S. Gardner, E.C. Moshopoulou, J.M. Mignot, M. Nicklas, W. Bao, N.O. Moreno, P.G. Pagliuso, I.N. Goncharenko, J.L. Sarrao, and J.D. Thompson, cond-mat/0307055 (unpublished).
[38] W. Bao (private Communication).
[39] J.S. Kim, J. Alwood, D. Mixson, P. Watts, and G.R. Stewart, Phys. Rev. B **66**, 134418 (2002).
[40] V.S. Zapf, N.A. Frederick, K.L. Rogers, K.D. Hof, P.-C. Ho, E.D. Bauer, and M.B. Maple, Phys. Rev. B **67**, 064405 (2003).
[41] H.v. Löhneysen, T. Pietrus, G. Portisch, H.G. Schlager, A. Schröder, M. Sieck, and T. Trappmann, Phys. Rev. Lett. **72**, 3262 (1994).
[42] G.R. Stewart, Rev. Mod. Phys. **73**, 797 (2001).
[43] W. Bao, G. Aeppli, J.W. Lynn, P.G. Pagliuso, J.L. Sarrao, M.F. Hundley, J.D. Thompson, and Z. Fisk, Phys. Rev. B **65**, 100505(R) (2002).
[44] B.M. McCoy and T.T. Wu, *Two Two-Dimensional Ising Model* (Harvard University Press, Cambridge, 1973).
[45] N.J. Curro, J.L. Sarrao, J.D. Thompson, P.G. Pagliuso, S. Kos, A. Abanov, and D. Pines, Phys. Rev. Lett. **90**, 227202 (2003).
[46] V.T. Rajan, Phys. Rev. Lett. **51**, 308 (1983).
[47] A. Bianchi, R. Movshovich, I. Vekhter, P.G. Pagliuso, and J.L. Sarrao, Phys. Rev. Lett. **91**, 257001 (2003).